



Eddy permitting simulations of freshwater injection from major Northern Hemisphere outlets during the last deglacial

Ryan Love¹, Heather Andres¹, Alan Condron², and Lev Tarasov¹

¹Department of Physics and Physical Oceanography, Memorial University of Newfoundland, St. John's, Newfoundland, Canada

²Geology & Geophysics, Woods Hole Oceanographic Institution, Woods Hole, Massachusetts, USA

Correspondence: Ryan Love (rlove@mun.ca)

Abstract. Freshwater, in the form of glacial runoff, is hypothesized to play a critical role in centennial to millennial scale climate variability such as the Younger Dryas and Dansgaard-Oeschger Events. Indeed, freshwater injection/hosing experiments with climate models have long shown that freshwater has the capability of generating such abrupt climate transitions. However, the relationship between freshwater and abrupt climate transitions is not straightforward. Large-scale glacial runoff events, such as Meltwater Pulse 1A, are not always temporally proximal to subsequent large-scale cooling. As well, the typical design of hosing experiments tends to artificially amplify the climate response. This study explores the impact that limitations in the representation of runoff in conventional hosing simulations has on our understanding of this relationship and addresses the more fundamental question of where coastally released freshwater is transported when it reaches the ocean. We focus particularly on the prior use of excessive freshwater volumes (often by a factor of 5) and present-day (rather than paleo) ocean gateways, as well as the injection of freshwater directly over sites of deep-water formation (DWF) rather than at runoff locations.

We track the routing of glaciologically-constrained freshwater volumes from four different plausible injection locations in a suite of eddy-permitting glacial ocean simulations using MITGCM under both open and closed Bering Strait conditions. Restricting freshwater forcing values to realistic ranges results in less spreading of freshwater across the North Atlantic and indicates that the response of DWF depends strongly on the geographical location of meltwater input. In particular, freshwater released into the Gulf of Mexico has little impact on DWF regions as a result of turbulent mixing by the Gulf Stream. In contrast, freshwater released from the Eurasian Ice sheet or initially into the Arctic is found to have the largest impact on DWF in the North Atlantic and GIN seas. Additional experiments show that when the Bering Strait is open, much like present-day, the Mackenzie River source exhibits twice as much freshening of the Labrador sea as a closed Bering Strait. Finally, our results illustrate that applying a freshwater 'hosing' directly into the North Atlantic with even "realistic" freshwater amounts still over-estimates the effect of terrestrial runoff on ocean circulation.

1 Introduction

The most recent deglacial and glacial periods are punctuated by large-scale centennial to millennial scale climate variability, including the Bølling-Allerød, Younger Dryas, and Dansgaard-Oeschger events. Changes in freshwater discharge into the ocean and subsequent transport are thought to play a significant role in this variability through their resultant impact on deepwater

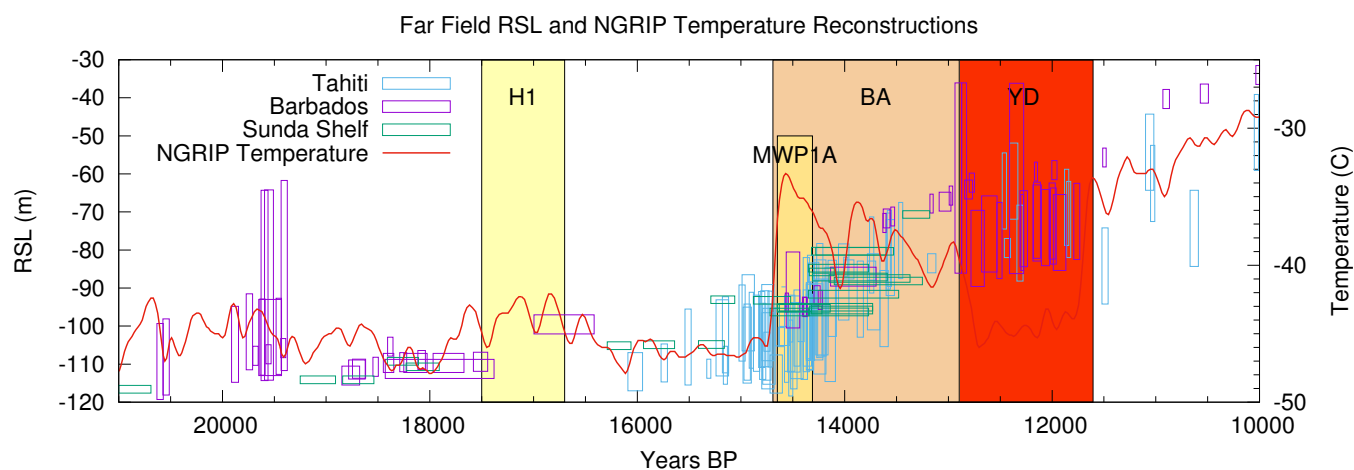


Figure 1. Far-field relative sea level records from Barbados (Fairbanks, 1989), Sunda Shelf (Hanebuth, 2000), and Tahiti (Deschamps et al., 2012) plotted along with a recent NGRIP temperature reconstruction for the deglacial (Kindler et al., 2014).

25 formation (DWF) in the North Atlantic (Broecker et al., 1989; Manabe and Stouffer, 1997; Teller et al., 2002). However, recent
earth system modelling (Peltier and Vettoretti, 2014; Zhang et al., 2014; Kleppin et al., 2015; Brown and Galbraith, 2016;
Vettoretti and Peltier, 2016; Zhang et al., 2017; Klockmann et al., 2018) has also demonstrated that changing freshwater inputs
into the oceans is not required to get such transitions. Furthermore, there are clear intervals during the last deglaciation when
strongly enhanced net freshwater injection into the oceans resulted in no temporally proximal cooling (see fig. 1). In the case
30 of MeltWater Pulse (MWP) 1-A, current best estimates of its timing indicate that, within dating uncertainties, the freshwater
injection coincides with the Bølling-Allerød (Deschamps et al., 2012) warm interval, as would be expected on physical grounds.
The more than millennial time interval to the onset of the subsequent cold Younger Dryas interval is beyond that permitting a
direct physical linkage.

The ability of freshwater to generate abrupt climate transitions has been supported by a myriad of hosing experiments, where
35 large volumes of freshwater ($1 - 10 \text{ decisiSverdrup}$, $1 \times 10^6 \text{ m}^3/\text{s} = 1 \text{ Sv} = 10 \text{ dSv}$) are imposed over sites of DWF (Kageyama
et al., 2013). Such hosings are meant to reproduce the effect of changing freshwater input into the oceans from regional ice
sheet melt and iceberg discharge as well as rerouting of surface runoff (Tarasov and Peltier, 2005). However, the climate model
support for this connection between freshwater injection and climate transitions is problematic given at least three common
experimental design problems.

40 The first issue is the geographic distribution of freshwater injection. Given the transport mechanisms of coastally released
freshwater, eg. boundary currents and mesoscale eddies (Condrón and Winsor, 2012; Hill and Condrón, 2014; Nurser and
Bacon, 2014), are well below the resolution of commonly used models, many studies opt to bypass the transport by injecting
freshwater directly onto sites of DWF (eg. Manabe and Stouffer (1997); Peltier et al. (2006); Otto-Bliesner and Brady (2010)).
Often-times the freshwater is introduced directly over 50-70N or the Ruddiman/Ice-Rafted-Debris (IRD) belt, a region of ocean
45 approximately between 40N and 50N in the North Atlantic, situated between Newfoundland, Canada and Portugal. These most



common injection locations usually inhibit DWF through a persistent freshwater cap that results in near-immediate decreases in AMOC (Stouffer et al., 2006). This attempt to compensate for coarse model resolution via hosing is problematic, since it assumes that all of the freshwater reaches the near surface DWF zone intact. It is unclear if a more realistic representation of runoff routing would yield a similar freshwater signal at the zones of DWF. The only eddy-permitting and boundary-current resolving modelling of freshwater forcing from actual continental outlets to date under glacial boundary conditions suggests this is not the case (Condrón and Winsor, 2012; Lohmann et al., 2020). However both of these studies have design limitations which limit the interpretability of their results. The unstructured mesh of FESOM in Lohmann et al. (2020) has refined (but not quite eddy-permitting) grid resolution largely only over the Arctic ocean and at coastal boundaries but is unable to resolve the impact of mesoscale eddies on freshwater transport over the central North Atlantic. In order to offset the short one-year interval of injection, Condrón and Winsor (2012) relied on fluxes of freshwater (50dSv) that were more than a factor of 20 larger than estimates derived from glaciological modelling over the Younger Dryas (Tarasov and Peltier, 2005).

The use of unrealistic volumes of freshwater in injection experiments is the second significant issue we identify in modelling studies. The amount of freshwater which is injected tends to be excessive, often of the order of 10dSv (eg. Peltier et al. (2006)), rather than the 1.5–2.5dSv derived from glaciological data constraints or modelling efforts such as Tarasov and Peltier (2006); Tarasov et al. (2012). It is understood that varying scales of freshwater injection can elicit wide ranges in climate behaviour (Roche et al., 2009; Kageyama et al., 2013). A previous investigation covering a range of freshwater injection fluxes shows that the change in North Atlantic Deep Water (NADW) formation becomes less sensitive to the injection location as fluxes grow larger (Roche et al., 2009), due to an increasing amount of diffusive spread. Furthermore, results from Peltier et al. (2006); Stouffer et al. (2006) demonstrate that the rate of change in AMOC and Greenland surface air temperature is much stronger for a 10dSv injection compared to that of a 3dSv injection.

The combination of both of these experimental design limitations (ie. unrealistically large volumes of freshwater injection and injection directly onto sites of DWF) will likely amplify climate system response compared to that arising from freshwater injection consistent with inferences and geography. A key step to confidently determining the role of freshwater runoff in millennial scale climate oscillations is therefore an assessment of the amount of freshwater transported to sites of DWF in a model that adequately resolves oceanic transports and that is subject to geographically realistic injection of freshwater in amounts consistent with best available inferences. This study provides one of the first such assessments using freshwater injection amounts constrained by the output of a calibrated ensemble of glacial evolution (Tarasov et al. (2012) and ongoing work) applied to a range of plausible source regions in a suite of simulations that are eddy-permitting over all regions of freshwater transport except the Arctic, where mesoscale eddies tend to have spatial scales of $O(10\text{km})$ or less (Nurser and Bacon, 2014). Given the importance of specific freshwater injection locations, we separately examine freshwater transport from the major outlet regions for the Northern Hemisphere posited to be important for these types of climate transitions: the Mackenzie River (MAK), Fennoscandia (FEN), the Gulf of St. Lawrence (GSL), and the Gulf of Mexico (GOM).

While investigating the transport of freshwater from different outlets, we also conducted an additional experiment examining the impact of uncertainties in the state of the Bering Strait. While it is clear that the Bering Strait was closed at the time of MWP1-A, there is some evidence that it may have been open during the onset of the Younger Dryas (England and Furze,



2008) although the majority of available evidence indicates closure during this time (eg. Jakobsson et al., 2017). Hu et al. (2007, 2012, 2015) demonstrate that the transport of freshwater can be strongly affected by the state of the Bering Strait under various background climates, with the effect that a closed Bering Strait leads to a stronger AMOC. Also, when the strait is closed, freshwater injected into the 50-70N band remains in the Arctic Ocean longer and results in a delayed recovery of the AMOC from freshwater forcing. We explore the ambiguity of the Bering Strait for the one key injection region that may be most affected by its state, the MAK in the Canadian Arctic.

2 Experimental Design

All of the simulations were performed using the Massachusetts Institute of Technology General Circulation Model (MITGCM) coupled sea-ice/ocean model in a Cubed-Sphere 6x510x510 (CS510) configuration, which provides $\approx 18\text{km}$ spatial resolution globally. This grid geometry and resolution is eddy-resolving to eddy-permitting for all ocean regions equatorialward of 60° (Chelton et al., 1998; Nurser and Bacon, 2014). This means it is able to capture small-scale phenomena like coastal boundary currents and mesoscale eddies that are among the primary mechanisms responsible for transport of terrestrial meltwater discharged into coastal, near-shore, environments (Condrón and Winsor, 2012; Hill and Condrón, 2014). Most of the coarser resolution models used in current and previous PMIP and CMIP working groups are unable to do this explicitly (Yang, 2003).

To conserve computation resources, the simulations presented here were initialized from the end of a previous $\approx 20\text{yr}$ LGM simulation using MITGCM and the same boundary conditions as Hill and Condrón (2014). The initial LGM simulation featured LGM bathymetry, sea level 120m lower than present, a glaciated Barents-Kara Sea and Canadian Archipelago, and a closed Bering Strait. The surface forcing used in that simulation includes winds, precipitation, 2m atmospheric temperatures, short and longwave radiation, surface runoff, and humidity from the CCSM3 working group's contribution to PMIP2 (Braconnot et al., 2007). We used the 3D ocean salinity and temperature fields from that MITGCM simulation to initialise two control runs with Younger Dryas bathymetry. To minimize computational resource requirements for spin-up, we kept the surface forcing the same as in the LGM simulation. Sea level was adjusted in both runs to that provided by the sea-level solver component of the Glacial Systems Model of Tarasov et al. (2012) at approx 13ka. The largest ensuing ocean gateway change compared to LGM is the opening up of the Barents-Kara Seas. The first control run features a closed Bering Strait as per the land ice reconstruction. The second control run was identical to the first except that the Bering Strait was opened to match its modern configuration. Opening the Barents-Kara Seas and the Bering Strait increases the flow into and out of the glacial Arctic Ocean.

The freshwater injection runs were branched from the tenth year of the control simulations, and all of the injection runs and the control simulations were then continued for an additional $\approx 10 - 20\text{yr}$. For the injection runs, 2dSv of freshwater were continually imposed to be an analogue for the outflow of solid and liquid mass from the Northern Hemisphere ice sheets. The ice sheet reconstruction (GLAC1-D Tarasov and Peltier (2005)) has the outflow of mass from the MAK outlet as largely icebergs until 19ka (so for our current configuration we can treat the outflow as mostly liquid) with no significant iceberg drainage for GSL and GOM. This assumption is not as applicable for flow of mass from the North American ice sheets directly into the Labrador Sea, where the majority of the discharge was in the form of icebergs until 11ka (at least in the data-constrained



glaciological modelling of Tarasov et al., 2012). The freshwater fluxes were determined by relying on two separate sources
115 of information: the glacial system model (GSM) from Tarasov et al. (2012) (the runoff chronology can be seen in fig. S1),
and other studies exploring realistic freshwater forcing during the Younger Dryas (such as Kageyama et al. (2013); Gong
et al. (2013)). To isolate geographic dependence, we test the effects that freshwater has when introduced at different locations
independently. We used the MAK outlet (as in Condron and Winsor (2012)), the GOM, the GSL, and a region off the coast of
Norway in FEN. Figure 2 provides a map showing each injection outlet. Figure S2 shows the regions over which the salinity
120 averages are calculated as well as each injection outlet.

Our experimental design has two possibly significant limitations, of which the short duration of the integrations and issues
with the surface forcing are the most problematic. Including the spin-up time, the injection runs are at longest ≈ 30 yr due to
computational constraints. This is insufficient time to spin up the deeper regions of the ocean and is of the order of magni-
tude for spinning up the upper layers. Despite this lack of equilibration in the deep ocean, these simulations are of sufficient
125 duration to resolve surface transports of freshwater by the glacial ocean, which is our primary focus here. The Younger Dryas
surface forcing fields we use are monthly values derived from a coupled climate model configured for LGM using ICE-5G
boundary conditions. This ice sheet configuration has been shown to generate more zonal atmospheric circulation patterns than
more recent reconstructions of LGM ice sheets (Ullman et al., 2014), and LGM winds are expected to be stronger and more
southward-shifted over the North Atlantic than winds during the Younger Dryas (Andres and Tarasov, 2019; Löffverström and
130 Lora, 2017). These biases are expected to enhance zonal transport in the North Atlantic.

3 Results and Discussion

Our two control simulations are very similar, as is expected given they only differ in the state of the Bering Strait. An ex-
amination of the salinity fields in fig. 2 and the velocity fields in fig. S3 reveals that the Gulf Stream in both simulations is
highly zonal. This feature is likely due to the surface wind forcing as discussed in the Experimental Design section. The sea
135 ice extent is consistent between simulation years, with maxima varying between $15.75 - 16\text{km}^2$ for the closed Bering Strait
(CBS) simulation and $17 - 18\text{km}^2$ for the open Bering Strait (OBS) simulation. Of note is the large region of sea ice cover off
the eastern coast of North America, extending as far south as 40N in the winter (see fig. 2 and figs. S3 and S4). The absence
of corresponding sea ice cover over the eastern North Atlantic indicates that there is substantial surface heat transport to this
region. Both the GIN and Labrador seas are covered with sea ice during the winter. Due to the extensive sea ice in this model,
140 the main DWF zone lies south of the sea ice edge, in the region between Greenland, Iceland, and the British Isles (see also fig.
S5). Mixed-layer depths in the Labrador sea region are much shallower than in the northern North Atlantic and indicate that
not much DWF is occurring there.

Since the focus of the current study is the surface transport of freshwater, coupled with the limited duration of these ex-
periments, we only discuss the immediate impact of freshwater on rates of DWF and AMOC here. The simulated state of the
145 AMOC is shown in fig. S6. The AMOC in the control simulations shows an overall similar structure but weaker values com-
pared to comparable high-resolution members of the multi-model, present-day ensemble in Hirschi et al. (2020). The strength

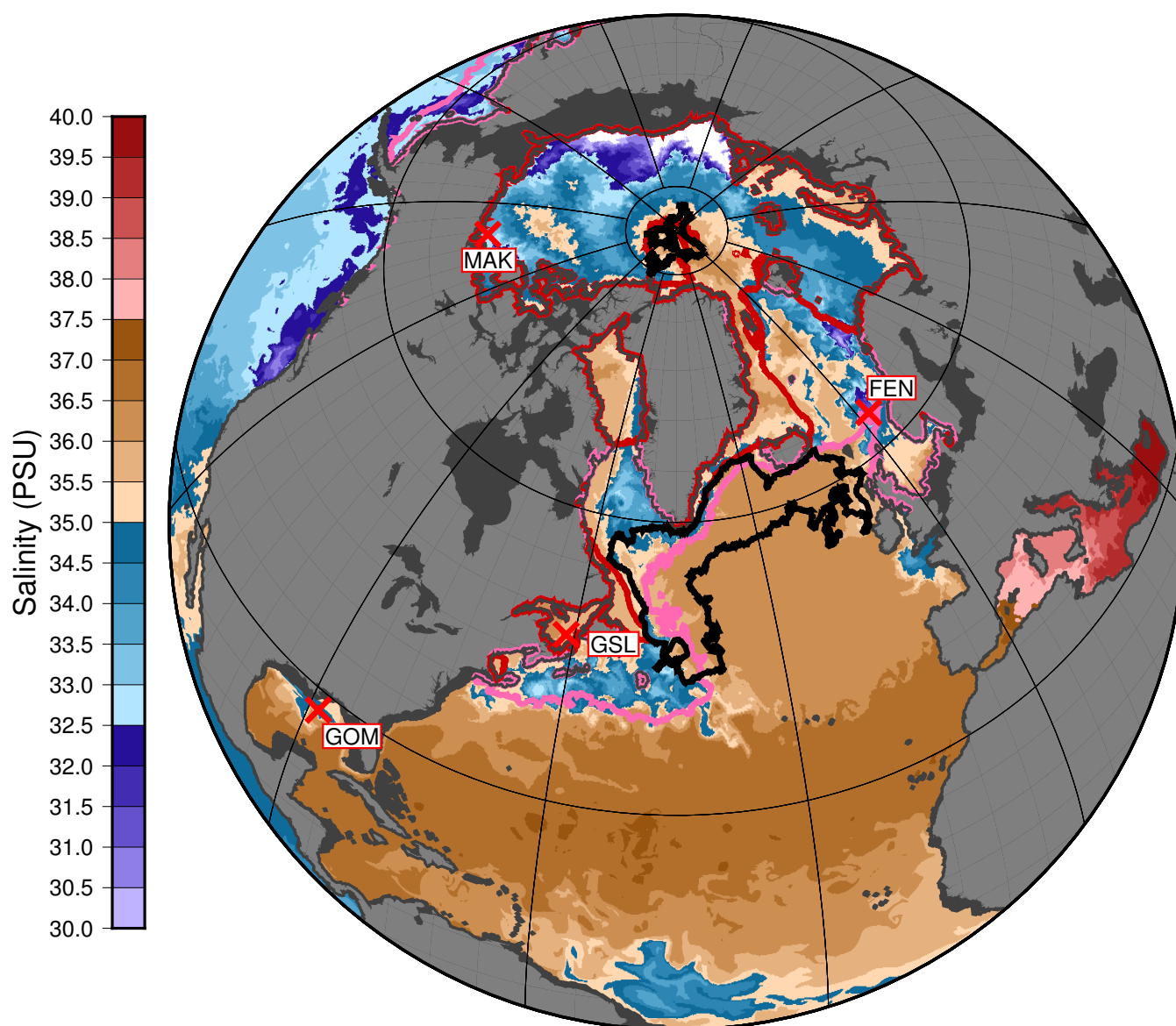


Figure 2. Sea surface salinity from a single day at the end of the CBS Control run. Present day land-sea mask is shown in light grey while simulation land-sea mask is contoured in a darker grey. The dark red and pink contours denote the time minimum and maximum sea ice extent respectively, of at least 15% sea ice coverage calculated over the last 5 years of the simulation. A 1000m mixed layer depth contour from the same time period as the sea ice extent contours is shown in black. Comparison of the sea ice maximal extent to the mixed layer depth shown in fig. S5 (for the OBS case) with the black contour in the current plot indicates that deep convection is just off the outer limit of the sea ice maximum. The strong zonality of the Gulf stream is readily visible in the salinity field. The eddy resolving/permitting nature of the model configuration is evident in the plotted salinity colour bands.

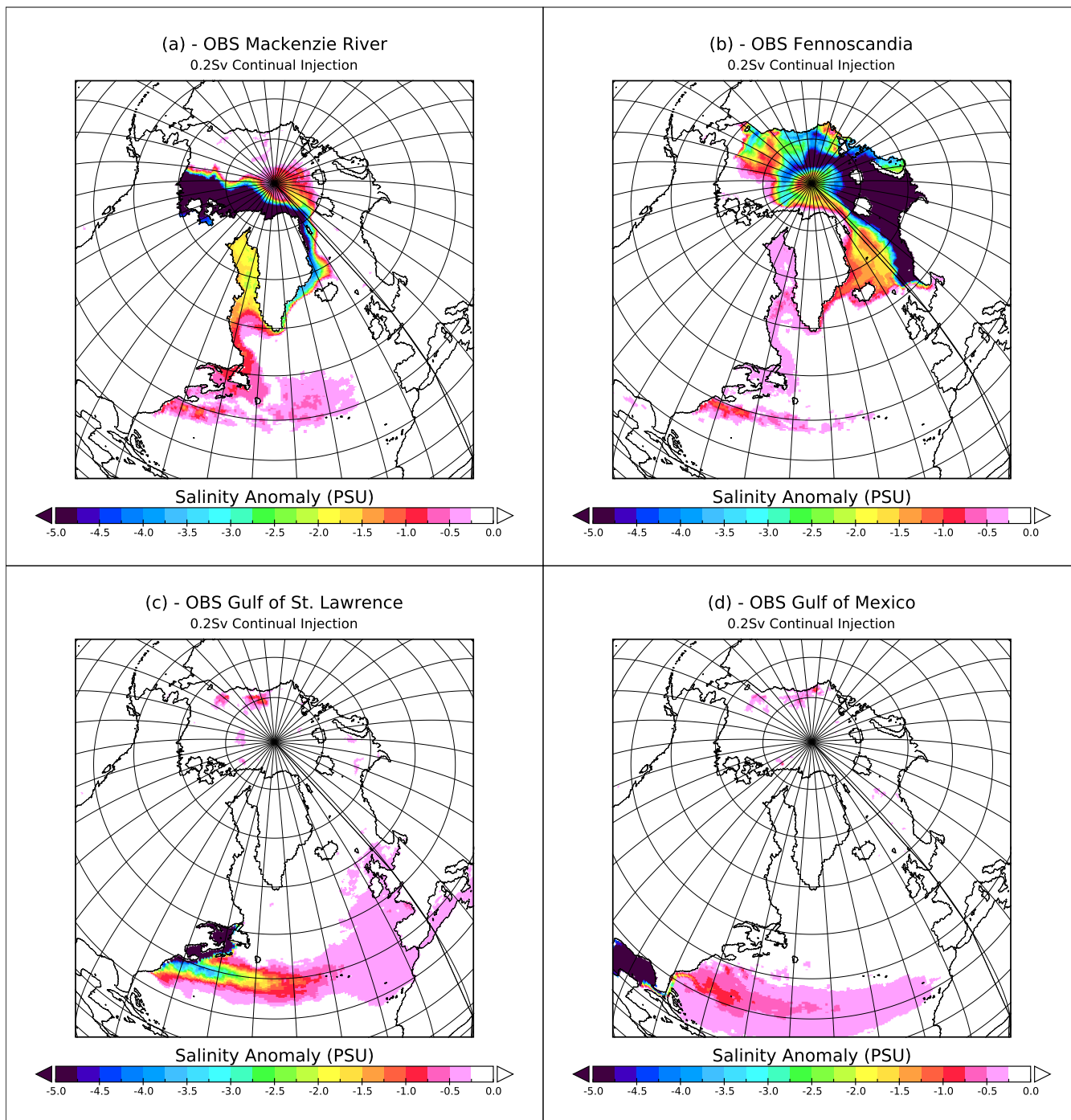


Figure 3. Time averaged sea surface salinity anomaly from the last 5 years of each of the OBS injection simulations, the CBS MAK experiment is available in the fig. S11.



of the AMOC at 26N in the control simulations is around 4Sv with a one-sigma annual variation of 1Sv, and a strong seasonality. Consistently with Hu et al. (2015), the CBS control run shows a stronger AMOC than OBS when examined using a 1 year running mean. However, unlike previous studies (e.g. Condrón and Winsor (2012)), freshwater forcing in the injection simulations does not influence the AMOC variability or the southward flow from the Labrador Sea above the threshold of internal variability on the time scales examined. The weak AMOC values obtained here indicate that the model is operating in a 'Glacial' mode relative to the previous study by Condrón and Winsor (2012), which showed AMOC values around 18Sv under present-day boundary conditions. The ocean operating in a glacial mode is reasonable given the glacial surface forcing and initialization conditions implemented here, although it is unlikely that in reality the ocean was in such a state just prior to the Younger Dryas (McManus et al., 2004). We expect that otherwise identical simulations performed using surface forcing and initialization conditions more consistent with the start of the Younger Dryas would generate more realistic AMOC values under both control and forcing conditions.

We begin our examination of the injection experiments by tracing the pathways of freshwater transport from each injection location. We present in fig. 3 salinity anomalies at the surface for each of the four injection locations. Figures S7, S8, S9, and S10 show the salinity anomalies at 50m, 100m, and 150m depth. These anomalies are calculated as the differences between averages over the last 5 years of the injection experiments and the corresponding 5 years of the relevant control simulation.

The path traced by freshwater injected at the mouth of the MAK when the Bering Strait is closed is shown in fig. S11. Due likely in good part to the lack of wind stirring given perennial sea ice cover, the bulk of the salinity anomaly is located at the surface. It fills the Canada basin, passes through Fram Strait along the continental shelf of Greenland, and follows the East Greenland Current southward from there. The concentration of freshwater in the surface current decreases dramatically as it travels to the West Greenland Current and into the Labrador Sea and Baffin Bay, although a significant signal is still detected along the path of the Labrador Current to the Gulf Stream. The large reduction in surface salinity anomaly along the east coast of Greenland coincides with the appearance of significant salinity anomalies at 100m depth and deeper. This is due to vertical mixing along the continental shelf of Greenland (with a local depth between 150-250m in this configuration) diluting the surface signature while introducing anomalies up to 200m depth.

While the freshwater pathway when the Bering Strait is open in fig. 3A and fig. S7 is broadly similar to that when it is closed, there are distinct features that provide insight into the mixing and transport processes occurring in a glacial ocean. Firstly, the Arctic surface salinity anomaly does not spread into the Canada Basin to the same degree, because it is constrained to lie between the Transpolar Current (not noticeably present in the CBS case) and the coast of the Canadian Archipelago. As a result, the surface freshwater concentrations carried along the East Greenland Current and West Greenland Current and into the Labrador Sea are much stronger than when the Bering Strait is closed. However, it is unclear that this contrast would persist if the simulation and injection were long enough to saturate accessible Arctic Ocean sectors. With an OBS there is less spreading into the subpolar gyre region and the Gulf Stream. When the Bering Strait is open there is a shift southward of the Gulf Stream and overall faster western boundary currents northwards and slower southwards of the Gulf Stream. Secondly, vertical mixing of the surface salinity anomaly appears to start earlier for the OBS case, in the shear zone of the Transpolar Current in the central Arctic. Thus, there is a stronger salinity anomaly at all depths to 150m off the north-eastern coast of

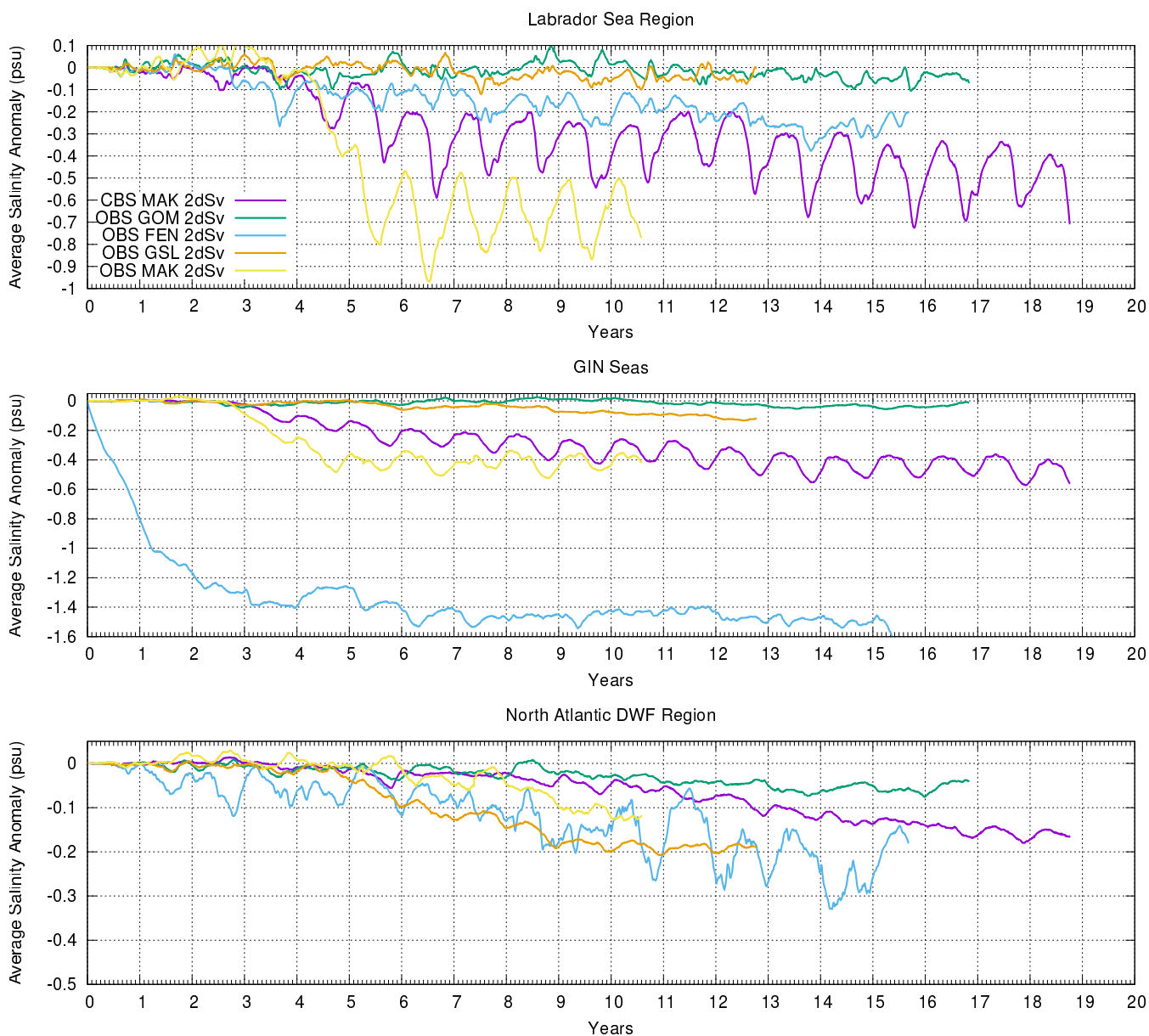


Figure 4. Sea surface salinity anomalies for each of our freshwater injection scenarios, calculated relative to their respective control runs. Each injection scenario uses 2dSv of freshwater continually injected at the location of their respective outlets. Each of the averaging regions is shown in the fig. S2.



Greenland for the OBS case. The primary differences in this pathway from what is observed and simulated for the present is that freshwater sourced from the MAK tends to flow eastward along the coastal margin into the Canadian Archipelago (Fichot et al., 2013; Condrón and Winsor, 2012), which is closed at the time of the Younger Dryas.

185 Freshwater from FEN tends to follow two different routes to DWF regions in fig. 3B and fig. S8. One freshwater mass travels directly across the GIN seas to eastern Greenland, following the surface currents shown in fig. S3. The second water mass is initially entrained in the Norwegian current, which carries the freshwater from the injection region northwards to flood the Barents-Kara sea. The freshwater then circles around the Arctic basin before being transported southwards back into the GIN seas and the North Atlantic via the East Greenland Current. Similarly to the MAK experiments, the freshwater from FEN
190 remains mostly in the top 50m of the water column until it reaches the continental margins of Greenland.

The freshwater from the GSL (fig. 3C and fig. S9) gets entrained in the Gulf Stream and only spreads meridionally on the eastern side of the North Atlantic, where it also becomes mixed vertically as it passes over the shallow (200-300m depth) continental margins. As previously noted, the Gulf Stream in our simulations is more zonal than during present day and may not accurately represent conditions just prior to the Younger Dryas. A more modern Gulf Stream, where surface currents are
195 more north-eastward, should result in greater freshwater transport to the North Atlantic DWF zone and GIN Seas, though again with substantial mixing.

Finally, freshwater released into the GOM initially fills that basin before leaking over the Florida shelf and into the Atlantic (see fig. 3D and fig. S10). Inflow from the Yucatán Channel acts as a barrier to the freshwater that has filled the GOM, preventing it from expanding southward. The lower sea level around the Younger Dryas results in a more isolated GOM relative to present
200 and helps to sequester the GOM from the Atlantic. As in the other scenarios, the freshwater remains in the uppermost layers as it passes over the Florida shelf. Afterwards, it mixes downward as it travels north and eventually becomes entrained in the Gulf Stream with freshwater present at least 200m deep. In neither the GSL nor the GOM injection is there evidence that the freshwater anomaly is able to cross the Gulf Stream as in Condrón and Winsor (2012). Furthermore, these simulations do not account for the effect of sediment in the glacial runoff which can lead to bottom-riding (hyperpycnal) flow in sufficient
205 concentrations (Parsons et al., 2001). Tarasov and Peltier (2005) suggested that outflow from the Mississippi (GOM) and the GSL at the magnitude studied here would be heavily laden with sediment, rendering the outflow hyperpycnal and dramatically changing the transport. By comparison, the MAK basin has limited surface sediments and freshwater outflow would be much less affected by this process.

Having traced the pathways of injected freshwater from each outlet, we now examine their respective contributions (fig. 4)
210 to three potential DWF regions: the Labrador Sea, GIN Seas and the northern North Atlantic. Labrador sea salinity is most strongly affected by freshwater injected into the MAK outlet, especially when the Bering strait is open. Closing the Bering Strait reduces this freshening effect to half, which makes it slightly stronger than the contribution from FEN. None of the other tested outlets contribute noticeably to salinity anomalies in the Labrador Sea. The GIN seas region is most significantly affected by freshwater from the FEN injection, whose salinity anomaly is five times larger than that from the next largest contributor, the
215 MAK. The reason for the importance of the FEN injection to GIN Seas salinity is largely due to its being within the averaging domain combined with the local ocean circulation directing FEN freshwater across the region.



Finally, the primary location of deep mixing in these simulations, the northern North Atlantic, is affected by injection into all of the outlets examined here. The strongest contribution is from the FEN injection, with a much larger seasonal cycle compared to that of the other tested outlets. The next strongest are the GSL and then the MAK, with the GSL appearing to have reached equilibrium. Neither the FEN nor MAK sourced simulations have reached apparent equilibration, making relative impact assessment for the latter uncertain in comparison with the GSL source simulation. By comparison, the CBS MAK appears to have equilibrated only at the end of the simulation (assuming the observed levelling off in the freshening effect is not a temporary hiatus) and the OBS case showing a slight downward trend. The CBS Mackenzie sourced simulation has a more delayed response compared to that of the corresponding OBS simulation as expected with the enhanced boundary currents observed with an OBS. This location of DWF has the longest equilibrium time around 10 – 15yr, with the sea surface timeseries for GIN and Labrador Seas shown in fig. 4 equilibrating within 5 – 10yr depending upon the outlet. Note that there is a detectable contribution to the salinity anomaly of the northern North Atlantic region from the GOM, although the salinity signal is not large enough in any single grid cell to be detectable in fig. S10. Of all our explored injection scenarios, the GOM scenario has the least impact with regards to salinity change in key DWF regions. The Mississippi River (primary meltwater drainage route to GOM) therefore offers a possible escape valve for minimizing the impact of terrestrial meltwater injection on DWF and therefore AMOC.

For comparison to conventional hosing studies, an order-of-magnitude calculation of the freshening effect of a 1-year 2dSv flux injected into each of the DWF regions (indicated in fig. S2) is worth consideration. We assume that the freshwater displaces existing seawater from the regions, that the injection region is evenly inundated with freshwater, and the freshwater is evenly mixed over the top 50m of the water column. We do not account for the eventual flow of water in or out of the regions. Using the salinity field from the control run as our initial state, hosing directly onto the Labrador sea region would result in a -4.2 PSU change in salinity, which is more than 4x stronger a freshening effect than any of our equilibrated injection runs. Hosing the GIN Seas region results in a -0.65 PSU salinity change, which is very similar to the top layer salinity shown in fig. 4 after 1 year of injecting into the FEN injection location (located within the GIN Seas region). Finally, hosing in the North Atlantic DWF region results in a -1.26 PSU salinity change. As in the Labrador Sea region, this represents an approximately 4x larger change than observed from any of the injection experiments presented herein.

Our results are broadly similar to those of Condron and Winsor (2012) and Hill and Condron (2014), which both featured a large 50dSv flux of freshwater for only the first year of the simulations. However, the much larger rate of freshwater injection in those studies generated much greater mixing at the boundaries of the coastal boundary currents and led to a greater spreading of the freshwater in the Arctic and Atlantic oceans. Also, the freshwater in Condron and Winsor (2012); Hill and Condron (2014) readily penetrates the Gulf Stream, routing freshwater from either the GSL or the Hudson Strait to south of Cape Hatteras and into the GOM and vice versa. An examination of the freshwater distributions in figs. S11 and S7 shows none of the overall flooding of the North Atlantic that is present in Condron and Winsor (2012). The lower but continual flux in the simulations shown here also does not allow freshwater to penetrate the Gulf Stream as in Condron and Winsor (2012). As such, the GSL injection delivers, relatively, significantly more freshwater to the GIN seas and North Atlantic DWF region than the GSL run in Condron and Winsor (2012) despite both a much lower flux and overall volume of freshwater.



Additionally, we can compare our results to Roche et al. (2009) and Lohmann et al. (2020). The former performed a wide suite of injection experiments using a much lower-resolution model with varying freshwater flux and injection location under LGM boundary conditions. The latter performed a set of 4 injection experiments using a model with enhanced grid resolution over large regions in the Arctic ocean and around the coasts while having the Atlantic grid resolution range upwards of 140km via their unstructured mesh approach. Since Roche et al. (2009) did not discuss the salinity signals at DWF sites directly, we interpret the freshening of the GIN Seas and northern North Atlantic DWF regions in this study to be analogous to changes in NADW export from their two sites of DWF. Our results are in broad agreement with both Roche et al. (2009) and Lohmann et al. (2020) except with regards to freshwater injected into the GOM. Roche et al. (2009) found their GOM injection to generate comparable or greater effects on NADW export than injection from the GSL. The freshwater signal at DWF sites in Lohmann et al. (2020) from GOM was also stronger than in this study. We attribute both differences to the lower resolutions of the Florida Strait and Gulf Stream in those studies (approximately 18 times coarser in Roche et al. (2009) and $\approx 2 - 3x$ coarser for Lohmann et al. (2020)). This lower resolution combined with the much longer duration of simulations in these studies would increase export rates and allow freshwater built up in the GOM time to flow out of the region and freshen the Atlantic. Finally, the higher resolution of the Gulf Stream in our set of simulations appears to make it a more effective barrier to freshwater transport than in either of these studies.

4 Conclusions

This study provides the first assessment of freshwater transport to deepwater formation regions under Younger Dryas conditions using realistic freshwater injection amounts applied to a range of plausible source regions in a suite of eddy-permitting simulations. We have addressed two main shortcomings in common practice for freshwater injection experiments that both inflate the salinity anomalies at locations of DWF. The first is the use of unrealistically large freshwater amounts. We find that limiting freshwater amounts to glaciologically-constrained values results in less diffusive spread of the freshwater across the North Atlantic. In addition, the lower amounts are unable to traverse the Gulf Stream, isolating the salinity anomalies introduced north and south of the Gulf Stream. The second shortcoming we address is the injection of freshwater directly over the locations of DWF rather than at its source location to mitigate unresolved $O(< 50\text{km})$ oceanic processes known to be important in the transport of glacial runoff. Using our model configuration, we find the transport of freshwater from the coast to sites of deepwater formation leads to a reduction in the effective freshwater forcing. We find in this study that a 2dSv injection at the mouth of the MAK (CBS) yields the equivalent of $\approx 0.32\text{dSv}$ of freshening in the Labrador Sea, $\approx 0.16\text{dSv}$ of freshening in the northern North Atlantic, and $\approx 1.2\text{dSv}$ in the GIN Seas compared to direct regional hosing after the first year. Thus, while this practice may mitigate the inability of coarse resolution models to adequately resolve the small-scale features that are key to freshwater transport, like boundary currents and mesoscale eddies, applying 2dSv directly into these regions is an inaccurate representation of the processes involved. Since non-eddy-permitting models are currently and will likely continue to be used for paleoclimate studies, we are presently exploring better ways to mitigate this problem.



We characterize which injection source region has the strongest freshening effect at three different potential deepwater formation (DWF) regions, the Labrador Sea, GIN Seas and northern North Atlantic. For climates where the dominant location of DWF is the northern North Atlantic, (most commonly occurring when the climate is in a glacial state with extensive sea ice (Braconnot et al., 2011)) freshwater introduced from FEN and the GSL imposes the largest freshening effect. In this circumstance, the effect of half as much freshwater from either of FEN or the GSL is equivalent to a single MAK sourced injection for the North Atlantic, assuming the freshwater transport scales approximately linearly with injection volume for changes of that order. For climate regimes where the dominant source of DWF is the Labrador Sea, freshwater from the MAK generates the greatest freshening, and this effect is doubled when the Bering Strait is fully open. Finally, for GIN Seas DWF, freshwater from FEN is by far the primary contributor to salinity anomalies.

Finally, we point out that the surface forcing used in the simulations was more consistent with LGM conditions than just prior to the Younger Dryas and was based on an obsolete reconstruction of ice sheet cover. We leave testing the representativeness of these results under more realistic surface forcing to future work.

Data availability. Model output data is available upon request.

Author contributions. All authors assisted with experimental design and analysis. RL prepared the manuscript with contributions from all authors.

Competing interests. The authors declare that they have no conflict of interest.

Acknowledgements. The authors would also like to thank those at the GNU and Fedora projects, Kernel.org and in particular those responsible for GNU Parallel (Tange, 2011) whose software greatly sped up and streamlined the analysis in this work. This research was enabled in part by support provided by SciNet (www.scinethpc.ca) and Compute Canada (www.computecanada.ca) through both Resources for Research Groups allocations and the Rapid Access Service. This is a contribution to the ArcTrain program, which was supported by the Natural Sciences and Engineering Research Council of Canada.



305 References

- Andres, H. J. and Tarasov, L.: Towards understanding potential atmospheric contributions to abrupt climate changes: characterizing changes to the North Atlantic eddy-driven jet over the last deglaciation, *Climate of the Past*, 15, 1621–1646, <https://doi.org/10.5194/cp-15-1621-2019>, 2019.
- Braconnot, P., Otto-Bliesner, B., Harrison, S., Joussaume, S., Peterchmitt, J.-Y., Abe-Ouchi, A., Crucifix, M., Driesschaert, E., Fichefet, T.,
310 Hewitt, C. D., and et al.: Results of PMIP2 coupled simulations of the Mid-Holocene and Last Glacial Maximum Part 1: experiments and large-scale features, *Climate of the Past*, 3, 261–277, <https://doi.org/10.5194/cp-3-261-2007>, 2007.
- Braconnot, P., Harrison, S., Otto-Bliesner, B., Abe-Ouchi, A., Jungclaus, J., and Peterschmitt, J.-Y.: The Paleoclimate Modeling Intercomparison Project contribution to CMIP5, *CLIVAR Exchanges*, 56, 15–19, 2011.
- Broecker, W. S., Kennett, J. P., Flower, B. P., Teller, J. T., Trumbore, S., Bonani, G., and Wolffi, W.: Routing of meltwater from the Laurentide
315 Ice Sheet during the Younger Dryas cold episode, *Nature*, 341, 318–321, <https://doi.org/10.1038/341318a0>, 1989.
- Brown, N. and Galbraith, E. D.: Hosed vs. unhosed: interruptions of the Atlantic Meridional Overturning Circulation in a global coupled model, with and without freshwater forcing, *Climate of the Past*, 12, 1663–1679, <https://doi.org/10.5194/cp-12-1663-2016>, 2016.
- Chelton, D. B., deSzoek, R. A., Schlax, M. G., El Naggar, K., and Siwertz, N.: Geographical Variability of the First Baroclinic Rossby Radius of Deformation, *Journal of Physical Oceanography*, 28, 433–460, [https://doi.org/10.1175/1520-0485\(1998\)028<0433:gvotfb>2.0.co;2](https://doi.org/10.1175/1520-0485(1998)028<0433:gvotfb>2.0.co;2),
320 1998.
- Condrón, A. and Winsor, P.: Meltwater routing and the Younger Dryas, *Proceedings of the National Academy of Sciences*, 109, 19928–19933, <https://doi.org/10.1073/pnas.1207381109>, 2012.
- Deschamps, P., Durand, N., Bard, E., Hamelin, B., Camoin, G., Thomas, A. L., Henderson, G. M., Okuno, J., and Yokoyama, Y.: Ice-sheet collapse and sea-level rise at the Bølling warming 14,600 years ago, *Nature*, 483, 559–564, <https://doi.org/10.1038/nature10902>, 2012.
- 325 England, J. H. and Furze, M. F.: New evidence from the western Canadian Arctic Archipelago for the resubmergence of Bering Strait, *Quaternary Research*, 70, 60–67, <https://doi.org/10.1016/j.yqres.2008.03.001>, 2008.
- Fairbanks, R. G.: A 17,000-year glacio-eustatic sea level record: influence of glacial melting rates on the Younger Dryas event and deep-ocean circulation, *Nature*, 342, 637–642, <https://doi.org/10.1038/342637a0>, 1989.
- Fichot, C. G., Kaiser, K., Hooker, S. B., Amon, R. M. W., Babin, M., Bélanger, S., Walker, S. A., and Benner, R.: Pan-Arctic distributions of
330 continental runoff in the Arctic Ocean, *Scientific Reports*, 3, <https://doi.org/10.1038/srep01053>, 2013.
- Gong, X., Knorr, G., Lohmann, G., and Zhang, X.: Dependence of abrupt Atlantic meridional ocean circulation changes on climate background states, *Geophysical Research Letters*, 40, 3698–3704, <https://doi.org/10.1002/grl.50701>, 2013.
- Hanebuth, T.: Rapid Flooding of the Sunda Shelf: A Late-Glacial Sea-Level Record, *Science*, 288, 1033–1035, <https://doi.org/10.1126/science.288.5468.1033>, 2000.
- 335 Hill, J. C. and Condrón, A.: Subtropical iceberg scours and meltwater routing in the deglacial western North Atlantic, *Nature Geoscience*, 7, 806–810, <https://doi.org/10.1038/ngeo2267>, 2014.
- Hirschi, J. J., Barnier, B., Böning, C., Biastoch, A., Blaker, A. T., Coward, A., Danilov, S., Drijfhout, S., Getzlaff, K., Griffies, S. M., and et al.: The Atlantic Meridional Overturning Circulation in High-Resolution Models, *Journal of Geophysical Research: Oceans*, 125, <https://doi.org/10.1029/2019jc015522>, 2020.
- 340 Hu, A., Meehl, G. A., and Han, W.: Role of the Bering Strait in the thermohaline circulation and abrupt climate change, *Geophysical Research Letters*, 34, <https://doi.org/10.1029/2006gl028906>, 2007.



- Hu, A., Meehl, G. A., Han, W., Timmermann, A., Otto-Bliesner, B., Liu, Z., Washington, W. M., Large, W., Abe-Ouchi, A., Kimoto, M., and et al.: Role of the Bering Strait on the hysteresis of the ocean conveyor belt circulation and glacial climate stability, *Proceedings of the National Academy of Sciences*, 109, 6417–6422, <https://doi.org/10.1073/pnas.1116014109>, 2012.
- 345 Hu, A., Meehl, G. A., Han, W., Otto-Bliesner, B., Abe-Ouchi, A., and Rosenbloom, N.: Effects of the Bering Strait closure on AMOC and global climate under different background climates, *Progress in Oceanography*, 132, 174–196, <https://doi.org/10.1016/j.pocean.2014.02.004>, 2015.
- Jakobsson, M., Pearce, C., Cronin, T. M., Backman, J., Anderson, L. G., Barrientos, N., Björk, G., Coxall, H., de Boer, A., Mayer, L. A., and et al.: Post-glacial flooding of the Bering Land Bridge dated to 11 cal ka BP based on new geophysical and sediment records, *Climate of the Past*, 13, 991–1005, <https://doi.org/10.5194/cp-13-991-2017>, 2017.
- 350 Kageyama, M., Merkel, U., Otto-Bliesner, B., Prange, M., Abe-Ouchi, A., Lohmann, G., Ohgaito, R., Roche, D. M., Singarayer, J., Swingedouw, D., and et al.: Climatic impacts of fresh water hosing under Last Glacial Maximum conditions: a multi-model study, *Climate of the Past*, 9, 935–953, <https://doi.org/10.5194/cp-9-935-2013>, 2013.
- Kindler, P., Guillevic, M., Baumgartner, M., Schwander, J., Landais, A., and Leuenberger, M.: Temperature reconstruction from 10 to 120 kyr b2k from the NGRIP ice core, *Climate of the Past*, 10, 887–902, <https://doi.org/10.5194/cp-10-887-2014>, 2014.
- 355 Kleppin, H., Jochum, M., Otto-Bliesner, B., Shields, C. A., and Yeager, S.: Stochastic atmospheric forcing as a cause of Greenland climate transitions, *Journal of Climate*, 28, 7741–7764, <https://doi.org/10.1175/JCLI-D-14-00728.1>, 2015.
- Klockmann, M., Mikolajewicz, U., and Marotzke, J.: Two AMOC states in response to decreasing greenhouse gas concentrations in the coupled climate model MPI-ESM, *Journal of Climate*, 31, 7969–7985, <https://doi.org/10.1175/JCLI-D-17-0859.1>, 2018.
- 360 Löffverström, M. and Lora, J. M.: Abrupt regime shifts in the North Atlantic atmospheric circulation over the last deglaciation, *Geophysical Research Letters*, 44, 8047–8055, <https://doi.org/10.1002/2017gl074274>, 2017.
- Lohmann, G., Butzin, M., Eissner, N., Shi, X., and Stepanek, C.: Abrupt Climate and Weather Changes Across Time Scales, *Paleoceanography and Paleoclimatology*, 35, <https://doi.org/10.1029/2019pa003782>, 2020.
- Manabe, S. and Stouffer, R. J.: Coupled ocean-atmosphere model response to freshwater input: Comparison to Younger Dryas Event, *Paleoceanography*, 12, 321–336, <https://doi.org/10.1029/96pa03932>, 1997.
- 365 McManus, J. F., Francois, R., Gherardi, J.-M., Keigwin, L. D., and Brown-Leger, S.: Collapse and rapid resumption of Atlantic meridional circulation linked to deglacial climate changes, *Nature*, 428, 834–837, <https://doi.org/10.1038/nature02494>, 2004.
- Nurser, A. J. G. and Bacon, S.: The Rossby radius in the Arctic Ocean, *Ocean Science*, 10, 967–975, <https://doi.org/10.5194/os-10-967-2014>, 2014.
- 370 Otto-Bliesner, B. L. and Brady, E. C.: The sensitivity of the climate response to the magnitude and location of freshwater forcing: last glacial maximum experiments, *Quaternary Science Reviews*, 29, 56–73, <https://doi.org/10.1016/j.quascirev.2009.07.004>, 2010.
- Parsons, J. D., Bush, J. W. M., and Syvitski, J. P. M.: Hypertypcnal plume formation from riverine outflows with small sediment concentrations, *Sedimentology*, 48, 465–478, <https://doi.org/10.1046/j.1365-3091.2001.00384.x>, 2001.
- Peltier, W. R. and Vettoretti, G.: Dansgaard-Oeschger oscillations predicted in a comprehensive model of glacial climate: A "kicked" salt oscillator in the Atlantic, *Geophysical Research Letters*, 41, 7306–7313, <https://doi.org/10.1002/2014GL061413>, 2014.
- 375 Peltier, W. R., Vettoretti, G., and Stastna, M.: Atlantic meridional overturning and climate response to Arctic Ocean freshening, *Geophysical Research Letters*, 33, n/a–n/a, <https://doi.org/10.1029/2005GL025251>, 106713, 2006.
- Roche, D. M., Wiersma, A. P., and Renssen, H.: A systematic study of the impact of freshwater pulses with respect to different geographical locations, *Climate Dynamics*, 34, 997–1013, <https://doi.org/10.1007/s00382-009-0578-8>, 2009.



- 380 Stouffer, R. J., Yin, J., Gregory, J. M., Dixon, K. W., Spelman, M. J., Hurlin, W., Weaver, A. J., Eby, M., Flato, G. M., Hasumi, H., and et al.: Investigating the Causes of the Response of the Thermohaline Circulation to Past and Future Climate Changes, *Journal of Climate*, 19, 1365–1387, <https://doi.org/10.1175/jcli3689.1>, 2006.
- Tange, O.: GNU Parallel - The Command-Line Power Tool, ;login: The USENIX Magazine, 36, 42–47, <http://www.gnu.org/s/parallel>, 2011.
- 385 Tarasov, L. and Peltier, W.: Arctic freshwater forcing of the Younger Dryas cold reversal, *Nature*, 435, 662–665, <https://doi.org/10.1038/nature03617>, 2005.
- Tarasov, L. and Peltier, W.: A calibrated deglacial drainage chronology for the North American continent: evidence of an Arctic trigger for the Younger Dryas, *Quaternary Science Reviews*, 25, 659–688, <https://doi.org/10.1016/j.quascirev.2005.12.006>, 2006.
- Tarasov, L., Dyke, A. S., Neal, R. M., and Peltier, W.: A data-calibrated distribution of deglacial chronologies for the North American ice complex from glaciological modeling, *Earth and Planetary Science Letters*, 315–316, 30 – 40, <https://doi.org/http://dx.doi.org/10.1016/j.epsl.2011.09.010>, sea Level and Ice Sheet Evolution: A {PALSEA} Special Edition, 2012.
- 390 Teller, J. T., Leverington, D. W., and Mann, J. D.: Freshwater outbursts to the oceans from glacial Lake Agassiz and their role in climate change during the last deglaciation, *Quaternary Science Reviews*, 21, 879–887, 2002.
- Ullman, D. J., LeGrande, A. N., Carlson, A. E., Anslow, F. S., and Licciardi, J. M.: Assessing the impact of Laurentide Ice Sheet topography on glacial climate, *Climate of the Past*, 10, 487–507, <https://doi.org/10.5194/cp-10-487-2014>, 2014.
- 395 Vettoretti, G. and Peltier, W. R.: Thermohaline instability and the formation of glacial North Atlantic super polynyas at the onset of Dansgaard-Oeschger warming events, *Geophysical Research Letters*, 43, 5336–5344, <https://doi.org/10.1002/2016GL068891>, 2016.
- Yang, J.: On the importance of resolving the western boundary layer in wind-driven ocean general circulation models, *Ocean Modelling*, 5, 357–379, [https://doi.org/10.1016/s1463-5003\(02\)00058-6](https://doi.org/10.1016/s1463-5003(02)00058-6), 2003.
- Zhang, X., Prange, M., Merkel, U., and Schulz, M.: Instability of the Atlantic overturning circulation during Marine Isotope Stage 3, *Geophysical Research Letters*, 41, 4285–4293, <https://doi.org/10.1002/2014gl060321>, 2014.
- 400 Zhang, X., Knorr, G., Lohmann, G., and Barker, S.: Abrupt North Atlantic circulation changes in response to gradual CO₂ forcing in a glacial climate state, *Nature Geoscience*, 10, 518–524, <https://doi.org/10.1038/NGEO2974>, 2017.